INTERNATIONAL JOURNAL OF ROBUST AND NONLINEAR CONTROL
Int. J. Robust Nonlinear Control 2010; **20**:1176–1196
Published online 5 August 2009 in Wiley InterScience (www.interscience.wiley.com). DOI: 10.1002/rnc.1501

Robust observer–controller compensator design using the loop shaping design procedure and the algebraic method

An-Chen Lee*,†, Yi-Ren Pan and Yuan-Yong Huang

Department of Mechanical Engineering, National Chiao-Tung University, 1001 Ta-Hsueh Road, Hsinchu City, Taiwan

SUMMARY

This paper investigates robust observer-controller compensator design using Vidyasagar's structure (VS). VS has a unit matrix parameter H similar to the Q parameter for the Youla–Kucera parameterization. VS can be designed based on the left coprimeness of the central controller in the H_∞-loop shaping design procedure (H_∞-LSDP) and therefore can preserve the intrinsic properties of the H_∞-LSDP. This paper introduces algebraic methods to simplify the design of H in the VS controller by solving specific algebraic equations. In particular, the algebraic design of H can achieve two things. First, a dynamic H adjusts the tracking performance and yields the integral action. Second, a dynamic H rejects the input and output sinusoidal disturbances with known frequencies. These attributes are indications of the flexibility of the proposed method since the output-feedback controller design of the H_∞-LSDP cannot easily deal with such conditions. This paper discusses the achieved loop and the closed-loop behavior of the system with VS, and also gives two numerical examples. The first example shows that the proposed method results in a better design in many aspects than the resulting from H_∞-LSDP. The second example shows the application of the proposed method to rejecting input and output step disturbances, and input and output multiple sinusoidal disturbances, for which the H_∞-LSDP can hardly be used. Copyright © 2009 John Wiley & Sons, Ltd.

Received 12 August 2008; Revised 12 June 2009; Accepted 15 June 2009

KEY WORDS: Youla–Kucera parameterization; H_∞-loop shaping design procedure; left coprime factorization; tracking control; sinusoidal disturbance rejection

1. INTRODUCTION

The observer–controller compensator (OBC) has been widely used in control system design because of its great flexibility [1–10]. In 2001, Giua *et al.* [3] proposed an OBC for a three-degree-of-freedom overhead crane with a time-varying suspending rope. Pandian *et al.* [4] proposed design methods for the estimation of chamber pressure variables and a sliding-mode controller to control a cylinder actuator. Noijen *et al.* [5] proposed a state-feedback controller combined with an observer that estimated the orientation error based on available trajectory information and measurement of the position coordinates for a unicycle mobile robot system. Driessen and Duggirala [6] proposed an OBC for a relatively large class of systems with hysteresis, and Alazard and Apkarian [7] used the Youla–Kucera parameterization (YKP) to give arbitrary-order H_∞ or μ controllers. Gao and Ho [8] suggested that the YKP may be non-proper and

*Correspondence to: An-Chen Lee, Department of Mechanical Engineering, National Chiao-Tung University, 1001 Ta-Hsueh Road, Hsinchu City, Taiwan.
†E-mail: aclee@mail.nctu.edu.tw

Contract/grant sponsor: Republic of China National Science Council; contract/grant number: NSC 94-221-E-009-181

proposed a modified parameterization of all proper stabilizing compensators. Gao and So [9] proposed a unified doubly coprime factorization, which is applicable to both descriptor systems and state-space systems. Gao [10] developed a PD observer parameterization for descriptor systems using the coprime factorization technique. Vidyasagar's structure (VS) is an OBC with an observer observing the partial state and a controller with an H parameter [11, 12]. Instead of the Q parameter over the set of proper and stable real rational functions denoted by RH_∞ in the YKP of [13–15], this H parameter is a unit over the set of proper and stable real rational functions denoted by $\mathbf{U}(RH_\infty)$. On the other hand, applications using the H_∞-loop shaping design procedure (H_∞-LSDP) of [16–18] have been the subject of further study, e.g. [19–23]. Panagopoulos and Astrom [19] showed that traditional methods for the design of PID controllers can be related to the H_∞-loop shaping method. Zhu *et al.* [21] designed a robust power system stabilizer using H_∞-loop shaping approach. Schinstick *et al.* [22] applied H_∞-loop shaping method to linear motor stages and non-contacting machines control. Patra *et al.* [23] used the H_∞-loop shaping method to design a robust load frequency controller. Hence, applying the principle of the H_∞-loop shaping method to VS and relating VS to the H_∞-LSDP fulfills the specified robustness requirement for more powerful design.

The H_∞-LSDP is an open-loop shaping approach that follows the elementary open-loop shaping principles specifying the closed-loop objectives in terms of requirements on the open-loop singular values, denoted by $\sigma(\bullet)$. That is, for a plant G and a controller K, the controller design achieves the desired loop (and controller) gains in the appropriate range:

$$\underline{\sigma}(GK) \gg 1, \quad \underline{\sigma}(KG) \gg 1, \quad \underline{\sigma}(K) \gg 1 \tag{1}$$

in a low frequency range $[0, \omega_l]$ and

$$\bar{\sigma}(GK) \ll 1, \quad \bar{\sigma}(KG) \ll 1, \quad \bar{\sigma}(K) \leqslant \delta \tag{2}$$

in a high frequency range $[\omega_h, \infty]$ where δ is not too large. $\bar{\sigma}(\bullet)$ and $\underline{\sigma}(\bullet)$ denote the maximum and minimum singular values, respectively. Hence, such a controller design makes

$$\begin{aligned} &\bar{\sigma}((I+GK)^{-1}), \quad \bar{\sigma}((I+KG)^{-1}) \\ &\bar{\sigma}(K(I+GK)^{-1}), \quad \bar{\sigma}((I+GK)^{-1}G) \end{aligned} \tag{3}$$

small in $[0, \omega_l]$ for good performance, and

$$\bar{\sigma}(GK(I+GK)^{-1}), \quad \bar{\sigma}(K(I+GK)^{-1}G) \tag{4}$$

small in $[\omega_h, \infty]$ for good robustness.

Section 2 shows that VS itself is a simple scheme and its equivalent output-feedback controller has a subset of solutions to the YKP in terms of feedback properties. In comparison with the equivalent controller and the YKP, the VS observer can be derived from the left coprimeness of the central (output-feedback) controller. The different feedback solutions to VS from YKP are indicated, and the feedback and tracking properties for the H parameter in the VS are also presented. Section 3 reviews the H_∞-LSDP and describes the VS design procedure. The first step of the VS design procedure uses the pre- and post-weighting matrices to shape the nominal plant, as in the H_∞-LSDP. These weighting matrices can be constant or dynamic. Using constant weighting matrices can reduce the dimension of VS and increase the crossover frequency. The dynamic weighting matrices are used for the integral action with the phase-advance term so that the feedback system can reject step disturbances. The VS observer can then be designed from the left coprimeness of the central controller of the H_∞-LSDP for a strictly proper plant. For a specific performance, the final step uses algebraic methods to design the H parameter in the VS controller to obtain the controller. Algebraically designing H provides solutions to four cases: constant H yields the integral action, dynamic H yields the integral action with the phase-advance term, dynamic H adjusts the tracking performance and yields the integral action, and dynamic H rejects the input and output sinusoidal disturbances with known frequencies, according to the algebraic equations. A constant pre-weighting matrix W_1 and post-weighting matrix W_2 are considered in the first three cases. The first two cases for rejecting step disturbances can also be achieved by W_1 or W_2. The last two cases present the flexibility of VS since the output-feedback controller design of the H_∞-LSDP cannot easily cope with the sinusoidal disturbance

DOI: 10.1002/rnc

rejection and the tracking control. H can affect the robust stability in addition to performance. Thus, the observer design of VS inherits the properties of the controller in the H_∞-LSDP and preserves certain robust stability. The VS controller design provides a robust stability/performance tradeoff. Section 4 provides two numerical examples. The first considers the case of a VS design that uses a pre-weighting matrix to reject the step disturbance and H to adjust the robust stability and the step tracking response. The case is compared to the output-feedback of the H_∞-LSDP with and without a pre-filter. The second example is designed to reject the input–output sinusoidal and step disturbances using the H parameter and the post-weighting matrix, respectively. Section 5 provides the conclusions of this paper.

2. DISCUSSION OF VS

A nominal plant $G(s)$ is assumed to be a proper real rational matrix. $G(s)$ is said to have a doubly coprime factorization if $(N(s), M(s))$ and $(\tilde{N}(s), \tilde{M}(s))$ are a right coprime factorization (RCF) and a left coprime factorization (LCF) of $G(s)$, i.e. $G = NM^{-1} = \tilde{M}^{-1}\tilde{N}$, respectively, and $N(s)$, $M(s)$, $\tilde{N}(s)$, $\tilde{M}(s)$, $X_r(s)$, $Y_r(s)$, $X_l(s)$, and $Y_l(s)$ exist over RH_∞ such that

$$\begin{bmatrix} X_r & Y_r \\ -\tilde{N} & \tilde{M} \end{bmatrix} \begin{bmatrix} M & -Y_l \\ N & X_l \end{bmatrix} = \begin{bmatrix} M & -Y_l \\ N & X_l \end{bmatrix} \begin{bmatrix} X_r & Y_r \\ -\tilde{N} & \tilde{M} \end{bmatrix} = I \tag{5}$$

Viswanadham [11] and Vidyasagar [12] proposed the VS, the OBC of Figure 1(a), where the nominal plant $G(s)$ has an RCF, i.e. $G = NM^{-1}$; the observer composed of X_r and Y_r observes the 'internal state' z to be $\hat{z}$, and the controller $C_v(s)$ feeds $\hat{z}$ back. Moreover, r, d_i and d_o denote the command reference, input disturbance and output disturbance, respectively; y is the system output, and e_r and e_d are the internal signals.

The system of Figure 1(a) is internally stable [12] if and only if

$$M(s) + C_v(s) = H(s) \in \mathbf{U}(RH_\infty) \tag{6}$$

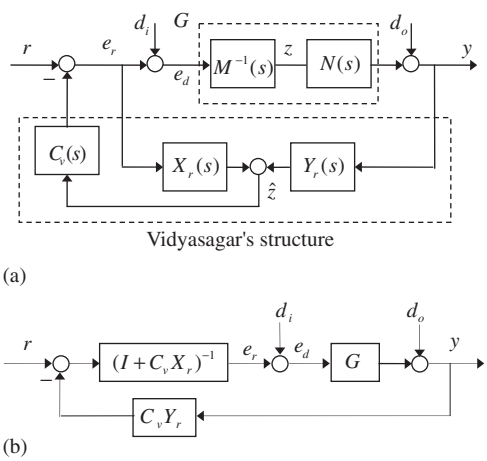

Figure 1. Vidyasagar's structure: (a) observer–controller compensator and (b) equivalent compensator.

The system of Figure 1(a) also can be transformed to the system of Figure 1(b) in terms of input–output equivalence. The notation $\mathbf{U}(RH_\infty)$ denotes a unit over RH_∞. When a square matrix and its inverse are stable, the matrix belongs to $\mathbf{U}(RH_\infty)$.

In terms of the feedback properties, the output-feedback controller $K_v(s) = (I + C_v X_r)^{-1} \cdot (C_v Y_r)$ in Figure 1(b) can be represented according to Equations (5) and (6) as

$$\begin{aligned} K_v(s) &= (I + C_v X_r)^{-1}(C_v Y_r) \\ &= [H^{-1}(I + C_v X_r)]^{-1}[H^{-1}(C_v Y_r)] \\ &= [X_r + H^{-1} Y_l \tilde{N}]^{-1}[Y_r - H^{-1} Y_l \tilde{M}] \end{aligned} \tag{7}$$

The YKP, all stabilizing controllers, can be parameterized as follows:

$$\begin{aligned} &K_{\mathrm{YK}}(s) = (X_r + Q\tilde{N})^{-1}(Y_r - Q\tilde{M}) \\ &Q(s) \in RH_\infty \text{ and } \det(I + Q\tilde{N}X_r^{-1})(\infty) \neq 0 \end{aligned} \tag{8}$$

When $Q(s)$ is zero, the result is the central controller of $K_{\mathrm{YK}}(s)$, $X_r^{-1}Y_r$. In comparison with X_r and Y_r of Equation (8), X_r and Y_r of Equation (7) play the similar role as central (output-feedback) controller, although H in Equation (7) cannot be zero. Nevertheless, this shows that the observer design of VS can be derived from the LCF of the central controller. Moreover,

DOI: 10.1002/rnc

the term $H^{-1}Y_l$ in Equation (7) corresponds to Q in Equation (8). This means that $K_v(s)$ is a subset of the YKP since H is a unit over RH_∞. However, VS is simpler than the YKP structure. Noted that VS in Figure 1(a) is stable itself while $K_v(s)$ of Equation (7) and $K_{\mathrm{YK}}(s)$ of Equation (8) are not necessarily stable.

VS is different from the YKP in terms of input–output relationships. The transfer functions from $(r, d_\mathrm{i}, d_\mathrm{o})$ to (e_r, e_d, y) in Figure 1(b) are as follows:

$$\begin{bmatrix} e_r \\ e_d \\ y \end{bmatrix} = \begin{bmatrix} MH^{-1} & M(X_r + H^{-1}Y_l\tilde{N}) - I & -M(Y_r - H^{-1}Y_l\tilde{M}) \\ MH^{-1} & M(X_r + H^{-1}Y_l\tilde{N}) & -M(Y_r - H^{-1}Y_l\tilde{M}) \\ NH^{-1} & N(X_r + H^{-1}Y_l\tilde{N}) & I - N(Y_r - H^{-1}Y_l\tilde{M}) \end{bmatrix} \begin{bmatrix} r \\ d_\mathrm{i} \\ d_\mathrm{o} \end{bmatrix} \quad (9)$$

Replacing $K_v(s)$ in Figure 1(b) with the YKP of Equation (8), produces transfer functions from $(r, d_\mathrm{i}, d_\mathrm{o})$ to (e_r, e_d, y),

$$\begin{bmatrix} e_r \\ e_d \\ y \end{bmatrix} = \begin{bmatrix} M & M(X_r + Q\tilde{N}) - I & -M(Y_r - Q\tilde{M}) \\ M & M(X_r + Q\tilde{N}) & -M(Y_r - Q\tilde{M}) \\ N & N(X_r + Q\tilde{N}) & I - N(Y_r - Q\tilde{M}) \end{bmatrix} \times \begin{bmatrix} r \\ d_\mathrm{i} \\ d_\mathrm{o} \end{bmatrix} \quad (10)$$

Even if Q in Equation (10) is replaced with $H^{-1}Y_l$, Equation (10) is still not equivalent to Equation (9) with respect to r. H exists in nine elements in Equation (9). The first column in Equation (9) corresponds to the tracking performance and the last two columns correspond to the feedback performance. This shows that H has both tracking and feedback properties. Finally, VS is more flexible than the central controller since the controller is included in VS [24].

3. COMPENSATOR DESIGN

This section uses the VS properties to obtain the observer directly from the LCF of the controller in the H_∞-LSDP in [17, 18]. This method ensures that the proposed VS design procedure is convenient and has the inherent properties of the H_∞-LSDP. The H_∞-LSDP is first reviewed below.

3.1. Review of the H_∞-LSDP

The H_∞-LSDP of [17, 18] incorporates the performance/robustness tradeoff obtained in loop shaping, with the guaranteed stability properties of the robust stabilization H_∞ problem [16]. The main results of [17, 18] are as follows.

The H_∞-LSDP uses a pre-weighting matrix W_1 and/or a post-weighting matrix W_2 to shape the singular values of the nominal plant G to the desired open-loop shape $G_S = W_2GW_1$. W_1 and W_2 are selected such that G_S has no hidden modes. The two weighting matrices can increase the loop gain and the crossover frequency, and/or introduce the integral action with or without the phase-advance term.

Then, the robust stabilization H_∞ problem is applied to the normalized RCF of G_S to produce a robust controller K_∞. Several researchers [12, 25–27] advocate an expression of coprime factor uncertainty in terms of additive stable perturbations to coprime factors of the nominal plant. Such a class of perturbations has advantages over additive or multiplicative unstructured uncertainty models. For example, the number of unstable zeros and poles may change as the plant is perturbed. That is, if the shaped plant is

$$G_S = N_S M_S^{-1} \quad (11)$$

a perturbed plant can be written as

$$G_\Delta = (N_S + \Delta_N)(M_S + \Delta_M)^{-1} \quad (12)$$

where M_S and N_S are the RCF of G_S, and Δ_M and Δ_N are stable, unknown transfer functions representing the uncertainty and satisfying $\left\| \begin{bmatrix} \Delta_N \\ \Delta_M \end{bmatrix} \right\|_\infty < \varepsilon$, where $\varepsilon(>0)$ presents the stability margin. The design objective is to find a feedback controller K_∞ that stabilizes all such

DOI: 10.1002/rnc

G_Δ for a given ε. Such a stabilizing controller K_∞ satisfies

$$\|M_S^{-1}(I+K_\infty G_S)^{-1}[K_\infty \;\; I]\|_\infty \leqslant \varepsilon^{-1} \tag{13}$$

Suppose the shaped plant of G_S has the minimal realization (A, B, C, D). A state-space construction for the normalized RCF can be obtained in terms of a solution to the generalized control (filter) algebraic Riccati equation as follows. The generalized control algebraic Riccati equation (GCARE) is

$$(A-BS^{-1}D^{\mathrm{T}}C)^{\mathrm{T}}X+X(A-BS^{-1}D^{\mathrm{T}}C) -XBS^{-1}B^{\mathrm{T}}X+C^{\mathrm{T}}R^{-1}C=0 \tag{14}$$

and generalized filter algebraic Riccati equation (GFARE) is

$$(A-BS^{-1}D^{\mathrm{T}}C)Z+Z(A-BS^{-1}D^{\mathrm{T}}C)^{\mathrm{T}} -ZC^{\mathrm{T}}R^{-1}CZ+BS^{-1}B^{\mathrm{T}}=0 \tag{15}$$

where $R \equiv I+DD^{\mathrm{T}}$, and $S \equiv I+D^{\mathrm{T}}D$. Then, the normalized RCF (M_S, N_S) is given as

$$\left[\begin{array}{c} M_S \\ \hline N_S \end{array}\right] = \left[\begin{array}{c|c} A+BF & BS^{-1/2} \\ \hline F & S^{-1/2} \\ \hline C+DF & DS^{-1/2} \end{array}\right] \tag{16}$$

where $F \equiv -S^{-1}(D^{\mathrm{T}}C+B^{\mathrm{T}}X)$. The normalized RCF of G_S means

$$M_S^{\mathrm{T}}(-\mathrm{j}\omega)M_S(\mathrm{j}\omega)+N_S^{\mathrm{T}}(-\mathrm{j}\omega)N_S(j\omega)=I \quad \text{for all } \omega \tag{17}$$

McFarlane and Glover [17] showed that a central controller satisfying Equation (13) can be obtained as follows:

$$K_\infty = \left[\begin{array}{c|c} A+BF+\gamma^2(W^{\mathrm{T}})^{-1}ZC^{\mathrm{T}}(C+DF) & -\gamma^2(W^{\mathrm{T}})^{-1}ZC^{\mathrm{T}} \\ \hline B^{\mathrm{T}}X & D^{\mathrm{T}} \end{array}\right] \tag{18}$$

where $W \equiv I+(XZ-\gamma^2 I)$ and γ are defined as $1/\varepsilon$. In addition, a maximum value of ε can be obtained by a non-iterative method, and is given by

$$\varepsilon_{\max} = \left(1-\left\|\begin{bmatrix} N_S \\ M_S \end{bmatrix}\right\|_H^2\right)^{1/2} \tag{19}$$

where $\|\bullet\|_H$ denotes the Hankel norm, and $\varepsilon_{\max}$ is the maximum stability margin. γ is always selected to be $\kappa/\varepsilon_{\max}$, where κ is a constant greater than zero. The final feedback controller K is constructed as $W_1 K_\infty W_2$.

3.2. VS design procedure

This section presents the VS design procedure and discusses only the strictly proper rational plant.

3.2.1. Selections of weighting matrices. The first step is to select the constant or dynamic weighting matrices W_1 and/or W_2 to shape the singular values of $G_S(= W_2 G W_1)$ as the LSDP does [17].

3.2.2. The design of the observer. The second step is to find an observer in VS. Suppose the shaped plant G_S has a minimal realization $[A, B, C, D]$ where $D=0$, and the perturbed shaped plant is presented by Equation (12). Then, according to Equation (16), the normalized RCF of G_S can be represented by

$$\left[\begin{array}{c} M_S \\ \hline N_S \end{array}\right] = \left[\begin{array}{c|c} A+BF & B \\ \hline F & I \\ \hline C & 0 \end{array}\right] \tag{20}$$

where $F=-B^{\mathrm{T}}X$. Theorem 1 shows that the observer composed of X_r and Y_r in VS can be derived from the LCF of the central controller in terms of feedback properties. Hence, the observer can be obtained from the LCF of the central controller in Equation (18), which satisfies Equation (13) with stability margin ε as follows:

$$\left[X_r \;\vdots\; Y_r\right] = \left[\begin{array}{c|c:c} A+QLC & B & -QL \\ \hline -F & I & 0 \end{array}\right] \tag{21}$$

DOI: 10.1002/rnc

where $Q=-\gamma^2(W^{\mathrm{T}})^{-1}$, $F=-B^{\mathrm{T}}X$ and $L=-ZC^{\mathrm{T}}$. Such an observer design preserves all advantages of the H_∞-LSDP in the design of VS. Moreover, the realizations of X_l, Y_l, $\tilde{N}_S$ and $\tilde{M}_S$ can be presented as follows:

$$[X_l \;\vdots\; Y_l]=\left[\begin{array}{c|c:c} A+BF & B & -QL \\ \hline C+DF & I & 0 \end{array}\right] \tag{22}$$

$$[\tilde{N}_S \;\vdots\; \tilde{M}_S]=\left[\begin{array}{c|c:c} A+QLC & B & QL \\ \hline C & 0 & I \end{array}\right] \tag{23}$$

where $\tilde{N}_S$ and $\tilde{M}_S$ are the LCF of G_S, but not the normalized LCF. Such coprime factorizations in Equations (20)–(23) satisfy Equation (24).

$$\begin{bmatrix} X_r & Y_r \\ -\tilde{N}_S & \tilde{M}_S \end{bmatrix}\begin{bmatrix} M_S & -Y_l \\ N_S & X_l \end{bmatrix} = \begin{bmatrix} M_S & -Y_l \\ N_S & X_l \end{bmatrix}\begin{bmatrix} X_r & Y_r \\ -\tilde{N}_S & \tilde{M}_S \end{bmatrix}=I \tag{24}$$

3.2.3. Design of H (the controller). The third step is to find the controller C_v in VS such that

$$\|M_S^{-1}(I+K_vG_S)^{-1}[K_v \;\; I]\|_\infty \leqslant \varepsilon_v^{-1}(=\gamma_v) \tag{25}$$

where $K_v=(I+C_vX_r)^{-1}C_vY_r$ and ε_v are the stability margin with respect to the shaped plant for the system with VS. The internal stability condition of Equation (8) can be rewritten as

$$M_S(s)+C_v(s)=H(s)\in\mathbf{U}(RH_\infty) \tag{26}$$

According to Equations (9), (24), and (26), Equation (25) can be written as Equation (27) or (28).

$$\|[H^{-1}C_vY_r \quad H^{-1}(I+C_vX_r)]\|_\infty \leqslant \varepsilon_v^{-1} \tag{27}$$

$$\|[Y_r-H^{-1}Y_l\tilde{M}_S \quad X_r+H^{-1}Y_l\tilde{N}_S]\|_\infty \leqslant \varepsilon_v^{-1} \tag{28}$$

Equation (28) shows that the H parameter in C_v can affect the value of the stability margin ε_v. Here, H is selected according to the control requirements and then the value of ε_v can be checked. H may require several redesigns to obtain a satisfactory value of ε_v.

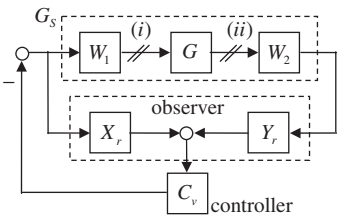

Figure 2. VS design procedure.

Remark 3.1

Equation (25) implicitly considers minimizing the H_∞ norm of the transfer functions from $(\tilde{d}_o, \tilde{d}_i)$ to (y_1, y_2) in Figure 3(a) as follows:

$$\begin{aligned}&\|M_S^{-1}(I+K_vG_S)^{-1}[K_v \;\; I]\|_\infty \\ &=\left\|\begin{bmatrix} I \\ G_S \end{bmatrix}(I+K_vG_S)^{-1}[K_v \;\; I]\right\|_\infty \\ &=\left\|\begin{bmatrix} W_1^{-1} \\ W_2G \end{bmatrix}(I+KG)^{-1}[KW_2^{-1} \;\; W_1]\right\|_\infty\end{aligned} \tag{29}$$

where the inner function $\begin{bmatrix} M_S \\ N_S \end{bmatrix}$ is pre-multiplied to go to the four-block problem. Corollary 1 of [18] shows that Equation (29) also equals Equation (30) by interchanging K_v and G_S:

$$\begin{aligned}&\|M_S^{-1}(I+K_vG_S)^{-1}[K_v \;\; I]\|_\infty \\ &=\left\|\begin{bmatrix} I \\ K_v \end{bmatrix}(I+G_SK_v)^{-1}[G_S \;\; I]\right\|_\infty \\ &=\left\|\begin{bmatrix} W_2 \\ W_1^{-1}K \end{bmatrix}(I+GK)^{-1}[GW_1 \;\; W_2^{-1}]\right\|_\infty\end{aligned} \tag{30}$$

Equation (30) presents the transfer functions from $(\tilde{d}_i, \tilde{d}_o)$ to (y_2, y_1) in Figure 3(b).

Equations (29) and (30) show how all the closed-loop objectives of Equations (3) and (4) are incorporated.

The following will show how to design H algebraically to achieve the four cases: constant H yields the integral action, dynamic H yields the integral action with the phase-advance term, dynamic H adjusts the

DOI: 10.1002/rnc

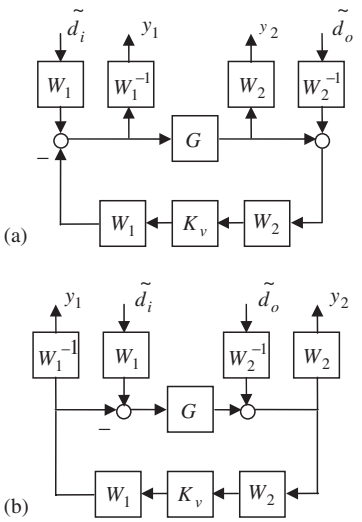

Figure 3. Two cases of the transfer functions from $(\tilde{d}_\mathrm{i}, \tilde{d}_\mathrm{o})$ to (y_1, y_2).

tracking performance and yields the integral action in the feedback system, and dynamic H rejects the input and output sinusoidal disturbances with known frequencies according to the algebraic equations.

The first case uses constant H to provide the integral action in the feedback system for the input and output disturbance rejections. If the disturbance is a step from the input and/or output of the plant, rejecting the disturbance requires that the Smith–Macmillan form of $W_1K_vW_2G$ [point (i) of Figure 2] and $GW_1K_vW_2$ [point (ii) of Figure 2] have a pole at 0 for every channel. If three conditions hold (W_1 and W_2 are constant, at least one channel of GY_r and Y_rG does not have any poles at 0, and K_v can be represented as $K_v=(C_v^{-1}+X_r)^{-1}Y_r$), then the requirements equal

$$(C_v^{-1}+X_r)|_{s=0}=0 \tag{31}$$

The third condition implies that the DC gain of C_v must not be a zero matrix so that Equation (31) equals

$$(I+C_vX_r)|_{s=0}=0 \tag{32}$$

Equation (32) presents the Smith–Macmillan in the form where the term $I+C_vX_r$ has a zero at 0 for every channel. The right-hand sides of Equations (31) and (32) are zero matrices with compatible dimensions.

The proof of Equation (32) is as follows. The transfer functions from the input disturbance to the output are

$$y=W_1N_SH^{-1}(I+C_vX_r)W_1^{-1}\cdot d_\mathrm{i} \tag{33}$$

When each element in the vector d_i is a unit step, each element in y indeed has a zero steady state according to Equation (32) and the final value theorem. Because of $H^{-1}(I+C_vX_r)=X_r+H^{-1}Y_l\tilde{N}_S$, Equation (33) can be rewritten as

$$y=W_1N_S(X_r+H^{-1}Y_l\tilde{N}_S)W_1^{-1}\cdot d_\mathrm{i} \tag{34}$$

Equations (33) and (34) show that the requirement of Equation (32) for the input step disturbance rejection also can be written as

$$(X_r+H^{-1}Y_l\tilde{N}_S)|_{s=0}=0 \tag{35}$$

since the DC gain of H must not be a zero matrix. Because of $X_l\tilde{N}_S=N_SX_r$ in Equation (24), Equation (35) can be rewritten as

$$(X_l+N_SH^{-1}Y_l)|_{s=0}=0 \tag{36}$$

Moreover, the transfer functions from the output disturbance to the output are

$$y=W_2^{-1}(X_l+N_SH^{-1}Y_l)\tilde{M}_SW_2\cdot d_\mathrm{o} \tag{37}$$

Hence, when each element in the vector d_o is a unit step, each element in y indeed has a zero steady state, according to Equation (36) and the final value theorem.

According to Equations (26) and (31), H in C_v should satisfy

$$H|_{s=0}=(M_S-X_r^{-1})|_{s=0} \tag{38}$$

Equation (38) shows that the simplest way to select H with integral action is

$$H=(M_S-X_r^{-1})|_{s=0} \tag{39}$$

There is only one requirement for the constant H in Equation (39) that makes the system's input and output unit step disturbances zero at the steady state.

The stability margin may be small, although Equation (39) leads to integral action in the feedback system and good step disturbance rejection at low frequencies. Hence, the second case will give the feedback system integral action with the phase-advance term using dynamic H to increase the stability margin.

DOI: 10.1002/rnc

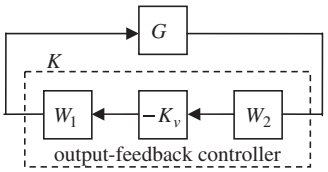

Figure 4. Positive output-feedback controller derived from VS.

Each channel in the open-loop shaping with a zero at $\phi_2(>0)$ can be achieved by satisfying

$$(C_v^{-1}+X_r)^{-1}|_{s=\phi_2}=0 \tag{40}$$

Equation (40) shows that the Smith–Macmillan form of the term $C_v^{-1}+X_r$ has a pole at ϕ_2 for each channel if the pole at ϕ_2 is not a hidden mode. Moreover, we assume that the Smith–Macmillan form of the term X_r does not have a pole at ϕ_2. Hence, the Smith–Macmillan form of the term C_v^{-1} must have a pole at ϕ_2 for each channel. That is, the term C_v has a zero at ϕ_2 for each channel so that the following equation is satisfied:

$$H|_{s=\phi_2}=M_S|_{s=\phi_2} \tag{41}$$

Thus, the integral action with the phase-advance term requires that H satisfy Equations (38) and (41). In that case, the element H_{ij} of the ith row and jth column in H can be selected as

$$H_{ij}(s)=h_{ij}\frac{s+k_{ij}}{s+p} \tag{42}$$

where the real number $p(>0)$ is given, and h_{ij} and $k_{ij}(>0)$ are selected according to Equations (38) and (41). This results in C_v. The final compensator can be in the form of the observer–controller configuration of Figure 2 or the (positive) output-feedback controller $K=-W_1K_vW_2$ of Figure 4.

W_1 and W_2 are assumed to be I in Figure 4. Rejecting the step input and output disturbance in VS requires that only parameter H satisfy Equations (38) and (41). This property of VS is better than that of the controller in the H_∞-LSDP, which may require W_1 and W_2 to improve the input and output step disturbances, respectively [17].

In the third case, H is used to adjust the tracking performance and produce the integral action in the feedback system. Suppose that the nominal plant has three inputs and three outputs, W_1 is an identity matrix, and W_2 is a constant matrix. To achieve unit step demand responses, the DC gain of the H parameter satisfies the final value theorem as follows:

$$\lim_{t\to\infty} y(t)=\lim_{s\to 0} sW_2^{-1}N_SH^{-1}\begin{bmatrix}1/s\\1/s\\1/s\end{bmatrix}$$

$$=\left(W_2^{-1}N_SH^{-1}\begin{bmatrix}1\\1\\1\end{bmatrix}\right)\Bigg|_{s=0}=\begin{bmatrix}1\\1\\1\end{bmatrix} \tag{43}$$

where y is the nominal plant output; N_S is obtained from the normalized RCF of $G_S(=N_SM_S^{-1})$; $W_2^{-1}N_SH^{-1}$ is the transfer function from step demands to y, and the step demands are a 3×1 vector with each element $1/s$. It is impossible for the DC gain of the H parameter to satisfy Equations (38) and (43). An extra constant matrix J is required to regulate the output responses and achieve the two objectives as follows:

$$\lim_{t\to\infty} y(t)=\lim_{s\to 0} sW_2^{-1}N_SH^{-1}J\begin{bmatrix}1/s\\1/s\\1/s\end{bmatrix}$$

$$=\left(W_2^{-1}N_SH^{-1}J\begin{bmatrix}1\\1\\1\end{bmatrix}\right)\Bigg|_{s=0}=\begin{bmatrix}1\\1\\1\end{bmatrix} \tag{44}$$

where the DC gain of H satisfies Equation (38). Introducing the constant J yields the final compensator in Figure 5, where r is the demand, y is the plant output, and d_i and d_o are the input and output disturbances, respectively.

The extra constant matrix J does not affect the open-loop shape, as shown in below

$$J(I+J^{-1}X_rC_vJ)^{-1}\cdot J^{-1}Y_r=(I+X_rC_v)^{-1}Y_r=K_v \tag{45}$$

DOI: 10.1002/rnc

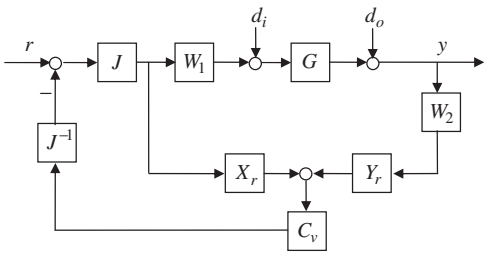

Figure 5. Control scheme of VS for tracking and step disturbance rejections.

If H is selected to be constant, as shown in Equation (39), the dynamic responses of the outputs depend only on N_S due to constants W_2 and J. However, N_S is often not sufficiently good to obtain satisfactory tracking performance. Hence, the dynamic H matrix is required and can be designed using

$$H^{-1}=\begin{bmatrix} h_1 & h_2 & h_3 \\ h_4 & h_5 & h_6 \\ h_7 & h_8 & h_9 \end{bmatrix}\cdot\frac{\det(N_S)}{\alpha(s)} \tag{46}$$

where $\det(N_S)$ is the determinant of N_S, the roots of the polynomial $\alpha(s)$ with the same orders as $\det(N_S)$ are designed in the left-half plane, and $h_1,\ldots,h_9$ can be obtained relying on the fact that the DC gains of H in Equations (38) and (46) are identical. The transfer function from r to y is then given by

$$y=W_2^{-1}\cdot\frac{\mathrm{Num}(N_S)}{\alpha(s)}\cdot\begin{bmatrix} h_1 & h_2 & h_3 \\ h_4 & h_5 & h_6 \\ h_7 & h_8 & h_9 \end{bmatrix}\cdot J\cdot r \tag{47}$$

where $\mathrm{Num}(N_S)$ is the numerator matrix of N_S. The term $\det(N_S)$ in Equation (46) can be chosen freely and has no effect on the tracking performance since it cancels. Equation (47) shows that $\alpha(s)$ can be designed to control the tracking performance. If the absolute values for the roots of $\alpha(s)$ are larger, the tracking response is faster but the system robustness is reduced. The robustness can be checked using Equation (B1). Thus, if the dynamic H matrix is designed as shown in Equation (36), the objectives of good step disturbance rejections and tracking performance can be achieved. H is designed in a similar way for other dimensions of the square or for wide plants.

Suppose that d_i and d_o are sinusoidal with frequencies at ω. If H is used to reject d_i and d_o, the following two equivalent equations must be satisfied according to Equations (34) and (37), respectively:

$$(X_r+H^{-1}Y_l\tilde{N}_S)|_{s=\mathrm{j}\omega}=0 \tag{48}$$

$$(X_l+N_SH^{-1}Y_l)|_{s=\mathrm{j}\omega}=0 \tag{49}$$

Equations (48) and (49) can be rewritten as Equations (50) and (51), respectively:

$$H|_{s=\mathrm{j}\omega}=-Y_l\tilde{N}_SX_r^{-1}|_{s=j\omega} \tag{50}$$

$$H|_{s=\mathrm{j}\omega}=-Y_lX_l^{-1}N_S|_{s=j\omega} \tag{51}$$

Because of $X_l\tilde{N}_S=N_SX_r$ in Equation (24), Equation (50) is equivalent to Equation (51). This means that the input and output sinusoidal rejections with a known frequency require only one of either Equation (50) or (51), which shows good VS properties. The following discussion uses Equation (50). Since each element for H at ω is a complex number, solving Equation (50) requires two unknown coefficients in each element of H. Hence, the ith row and jth column element of H can be given algebraically as

$$H_{ij}(s)=h_{ij1}+\frac{h_{ij2}}{s+p_h} \tag{52}$$

where $p_h(>0)$ is given, and h_{ij1} and h_{ij2} can be solved according to Equation (50). If the result of H is not unimodular, another value of p_h is given and Equation (50) is solved again. In a similar manner, if the input and output disturbances have two known sinusoidal frequencies, ω_1 and ω_2, then each element of H needs four coefficients to be solved as

$$H_{ij}(s)=h_{ij1}+\frac{h_{ij2}}{s+p_h}+\frac{h_{ij3}}{(s+p_h)^2}+\frac{h_{ij4}}{(s+p_h)^3} \tag{53}$$

The four coefficients for each element of H in Equation (53) are obtained according to Equation (50) with respect to ω at ω_1 and ω_2. That is, the number of the coefficients in $H_{ij}(s)$ to be solved is twice the number of the different frequencies.

DOI: 10.1002/rnc

The H in VS provides flexibility to the compensator. When designing H, it is straightforward to obtain solutions to the four cases described earlier. More complex H design methods are not presented here. For example, H adjusts the tracking performance and rejects the sinusoidal input disturbance simultaneously. Since H, W_1, or W_2 can achieve integral action with or without the phase-advance term, it is possible to implement the integral action using W_1 or W_2, and to solve other problems such as tracking control or sinusoidal disturbance with H.

3.3. Achieved loop shape

As described above, the desired loop shaped was specified as W_2GW_1, but the final shape of the loop achieved is in fact given by $W_1K_vW_2G$ at the plant input [point (i) of Figure 2] and $GW_1K_vW_2$ [point (ii) of Figure 2]. McFarlane and Glover [17] have suggested that if $\gamma(\equiv\varepsilon^{-1})$ is small enough, $\underline{\sigma}(G_S)$, is large enough at low frequencies, and $\bar{\sigma}(G_S)$ is small enough at high frequencies, then the deteriorations of the loop shapes $W_1K_\infty W_2G$ and $GW_1K_\infty W_2$ at low and high frequencies are limited for the H_∞-LSDP, according to Theorems A.1 and A.2, respectively. With the help of these results [17], this section shows that the deteriorations of the loop shapes $W_1K_vW_2G$ and $GW_1K_vW_2$ at low and high frequencies are also limited, according to Theorems 1 and 2, respectively.

The following equations show that $\underline{\sigma}(K_v)$ requires a bound on the deterioration of the loop shapes at low frequencies:

$$\begin{aligned}\underline{\sigma}(GK) &= \underline{\sigma}(GW_1K_vW_2)\\ &\geqslant \underline{\sigma}(W_2GW_1)\underline{\sigma}(K_v)/c(W_2) \qquad (54)\\ \underline{\sigma}(KG) &= \underline{\sigma}(W_1K_vW_2G)\\ &\geqslant \underline{\sigma}(W_2GW_1)\underline{\sigma}(K_v)/c(W_1) \qquad (55)\end{aligned}$$

where the designer can select the condition numbers $c(W_1)$ and $c(W_2)$. The following result shows that $\underline{\sigma}(K_v)$ is bounded by $\underline{\sigma}(X_r^{-1}Y_r)$, $\underline{\sigma}(C_v)$, and $\underline{\sigma}(X_r)$, and hence by Equations (54) and (55), and the high gain of $\underline{\sigma}(C_v)$ limits the deterioration of K_v at low frequencies.

Theorem 1
At frequencies of high loop gain, the smallest singular value of the controller C_v should increase since

$$\underline{\sigma}(K_v)\geqslant\frac{\underline{\sigma}(X_r^{-1}Y_r)}{1+\dfrac{1}{\underline{\sigma}(C_v)\underline{\sigma}(X_r)}} \qquad (56)$$

Proof
Equation (56) follows from simple manipulation of singular value inequalities. □

$\underline{\sigma}(X_r^{-1}Y_r)$ in Equation (56) is the smallest singular value of the central controller K_∞ in Equation (18), and is large enough if γ is small enough and $\underline{\sigma}(G_S)$ is large enough at low frequencies, according to Theorem A.1. Hence, for such K_∞, K_v is large enough if $\underline{\sigma}(C_v)$ is large enough. Then, $\underline{\sigma}(GK)$ or $\underline{\sigma}(KG)$ are also large enough at low frequencies according to Equations (54) and (55).

The following equations show that $\bar{\sigma}(K_v)$ requires a bound on the deterioration of the loop shapes at high frequencies:

$$\begin{aligned}\bar{\sigma}(GK) &= \bar{\sigma}(GW_1K_vW_2)\\ &\leqslant \bar{\sigma}(W_2GW_1)\bar{\sigma}(K_v)c(W_2) \qquad (57)\\ \bar{\sigma}(KG) &= \bar{\sigma}(W_1K_vW_2G)\\ &\leqslant \bar{\sigma}(W_2GW_1)\bar{\sigma}(K_v)c(W_1) \qquad (58)\end{aligned}$$

In a similar manner, the following result shows that $\bar{\sigma}(K_v)$ is bounded by $\bar{\sigma}(X_r^{-1}Y_r)$, $\bar{\sigma}(C_v)$, and $\bar{\sigma}(X_r)$, and hence by Equations (57) and (58), while the low gain of $\bar{\sigma}(C_v)$ limits the deterioration of K_v at high frequencies.

Theorem 2
At frequencies of low loop gain, the largest singular value of the controller C_v should decrease because

$$\bar{\sigma}(K_v)\leqslant\frac{\bar{\sigma}(X_r^{-1}Y_r)}{\dfrac{1}{\bar{\sigma}(C_v)\bar{\sigma}(X_r)}-1} \qquad (59)$$

Proof
Equation (59) follows from simple manipulation of singular value inequalities. □

DOI: 10.1002/rnc

$\bar{\sigma}(X_r^{-1}Y_r)$ in Equation (59) is the largest singular value of the central controller K_∞ in Equation (18), and is small enough if γ is small enough and $\bar{\sigma}(G_S)$ is small enough at high frequencies according to Theorem A.2. Hence, for such K_∞, K_v is small enough if $\bar{\sigma}(C_v)$ is small enough. Then, either $\bar{\sigma}(GK)$ or $\bar{\sigma}(KG)$ is also small enough at high frequencies according to Equations (57) and (58).

This section shows that the selections of K_∞ and C_v can affect the singular values of K_v. Moreover, W_1, W_2, and C_v can be used to set the performance/robustness tradeoff so that Equation (25) is satisfied.

3.4. Closed-loop behavior

The H_∞-LSDP in [17] ensures that a number of standard closed-loop design objectives are bounded. According to Equations (30) and (31), Theorem 4.2 in [17] can be rewritten as Theorem B.1. Theorem B.1 shows that the bounds on the behavior of all closed-loop transfer functions of Equations (3) and (4) depend on the normalized RCF or normalized LCF of $G_S = W_2 G W_1$, γ_v, W_1, and W_2. Hence, the closed-loop objectives of the VS are also 'well behaved', as they are referred to by McFarlane and Glover [17].

The trade-off between stability and performance can be seen in Equations (B1)–(B7). When fewer task requirements are required of H, more-complex W_1 and/or W_2 is/are needed and $c(W_1)$ and/or $c(W_2)$ are larger (bigger than one). Then, to satisfy Equations (B1)–(B7), γ_v will be smaller since $c(W_1)$ and/or $c(W_2)$ will be larger (greater than one). Hence, when fewer task requirements are placed on H, the stability margin is larger, and vice versa.

4. TWO DESIGN EXAMPLES

Example 1

This example applies to the proposed VS design procedure for designing a robust compensator for the aircraft model AIRC [17]. Algebraic methods are proposed for the input and output step disturbance rejection and the tracking performance. The robust VS compensator is compared with the H_∞-LSDP controller.

The model used in a linearized model of the vertical-plane dynamics of an aircraft with three inputs, three outputs, and five states. The inputs are spoiler angle (u_1 measured in tenths of a degree), forward acceleration (u_2 in m/s^2), and elevator (u_3 in degrees). The states are altitude relative to some datum (x_1 in m), forward speed (x_2 in m/s), pitch angle (x_3 in degrees), pitch rate (x_4 in degree/s), and vertical speed (x_5 in m/s). The three outputs (y_1, y_2, y_3) are just the first three states (x_1, x_2, x_3), which are to be controlled. The continuous-time state-space matrices of the nominal plant are listed in Appendix C. The plant has no transmission zeros and has poles located at -0.78 ± 1.03j, -0.0176 ± 0.1826j and 0.

The design requirements are to achieve a crossover frequency of about 10 rad/s, with reasonably damped responses and zero steady-state error in the face of step demands or disturbances.

VS Design Procedure:

Step 1. The dynamic pre-weighting matrix W_1 is selected as

$$W_1 = \text{diag}\left\{\frac{24(s+0.4)}{s}, \frac{12(s+0.4)}{s}, \frac{24(s+0.4)}{s}\right\} \quad (60)$$

to increase the crossover frequency and reject the input and output disturbances. W_2 is an identity matrix.

Step 2. An eighth-order controller K_∞ of Equation (18) satisfying Equation (13) ($\varepsilon = 0.361$) is obtained. X_r and Y_r, the LCF of K_∞, are derived from Equation (21). The observer composed of X_r and Y_r is obtained in Appendices D.1 and D.2.

Step 3. The controller (C_v) is designed. The normalized RCF of the shaped plant $G_S(s)(=G(s)W_1(s))$ is $(N_S(s), M_S(s))$. $N_S(s)$ has poles at -12.2268, -0.4001, -7.6683 ± 7.6322j and -2.3696 ± 2.3435j. Then, the transfer function from r to y in Figure 5 is as follows:

$$y = W_2^{-1} N_S H^{-1} J \cdot r \quad (61)$$

where W_2 is an identity matrix. If H^{-1} is selected to be

$$H^{-1}(s) = \text{diag}\left\{\frac{0.1(s+12.2268)}{s+5}, \frac{0.1(s+12.2268)}{s+5}, \frac{0.1(s+12.2268)}{s+5}\right\} \quad (62)$$

DOI: 10.1002/rnc

then the stable zero of $H^{-1}(s)$ at -12.2268 cancels the stable pole of $N_S(s)$, which can reduce the control effort on r. Moreover, the value of the coefficient, 0.1, in each element of H^{-1} can increase the stability margin according to Equation (28). The system stability margin ε_v is 0.326. When the coefficient is near zero, ε_v will be close to ε. If the value of the coefficient is larger, the value of ε_v will be smaller. For example, the stability margin is 0.165 when the value of the coefficient is 1. Therefore, $H(s)$ requires several designs to obtain a satisfactory value of ε_v. This is the disadvantage of the VS design procedure. Moreover, a constant matrix J for regulating the output final values is given by

$$J=\begin{bmatrix} -2.4661 & -0.3402 & 3.2443 \\ -0.2276 & 4.0751 & 0.2544 \\ -3.2542 & -0.0272 & -2.4764 \end{bmatrix} \tag{63}$$

The M_S of Appendix D.3 and designed H and C_v are obtained according to Equation (26). Then, the final (negative) feedback controller $K=W_1K_v$ is obtained. Figure 6(a) and (b) show the singular values of the open loops, GK and KG, respectively; their crossover frequencies are about 10 rad/s. Figure 7(a) and (b) shows the output and input sensitivity functions with the largest peak values of 1.57 and 1.58, respectively. Figure 8(a) and (d) shows the output responses and control inputs, respectively, for demands with $(1/s, 0, 0)$. Figure 8(b) and (e) shows the output responses and control inputs, respectively, for demands with $(0, 1/s, 0)$. Figure 8(c) and (f) shows the output responses and control inputs, respectively, for demands with $(0, 0, 1/s)$. Figure 8 demonstrates that the outputs have almost no overshoots, the interaction between outputs is less than 20%, and the control inputs are limited as follows:

$$u_1<10^\circ, \quad u_2<5\,\mathrm{m/s}, \quad u_3<10^\circ$$

Comparison with the H_∞-LSDP

McFarlane and Glover [17] designed this example with W_2 as follows:

$$W_2=\mathrm{diag}\left\{\frac{24(s+0.4)}{s}, \frac{12(s+0.4)}{s}, \frac{24(s+0.4)}{s}\right\} \tag{64}$$

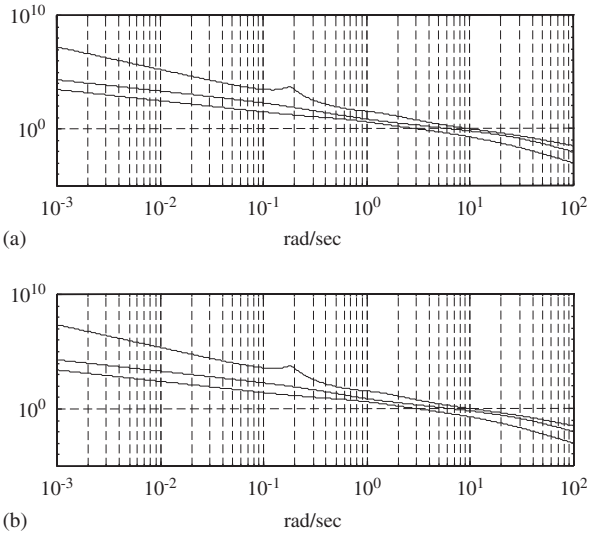

Figure 6. Singular values of (a) GK and (b) KG.

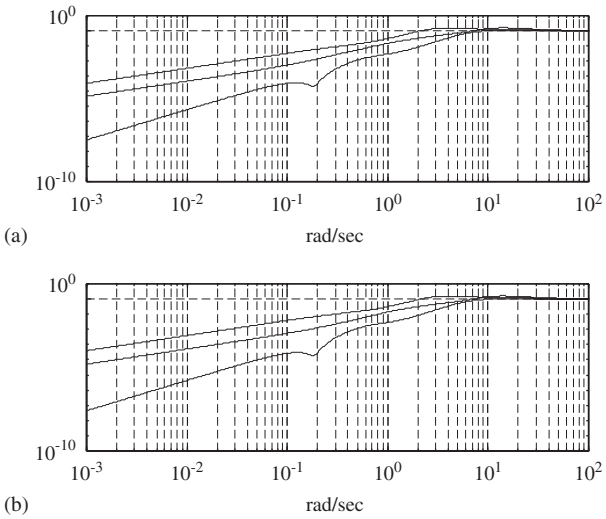

Figure 7. Singular values of (a) output sensitivity function and (b) input sensitivity function.

Here, the final controller $K=K_\infty W_2$ of the H_∞-LSDP is obtained with no model reduction. The stability margin ε of the H_∞-LSDP is 0.361.

DOI: 10.1002/rnc

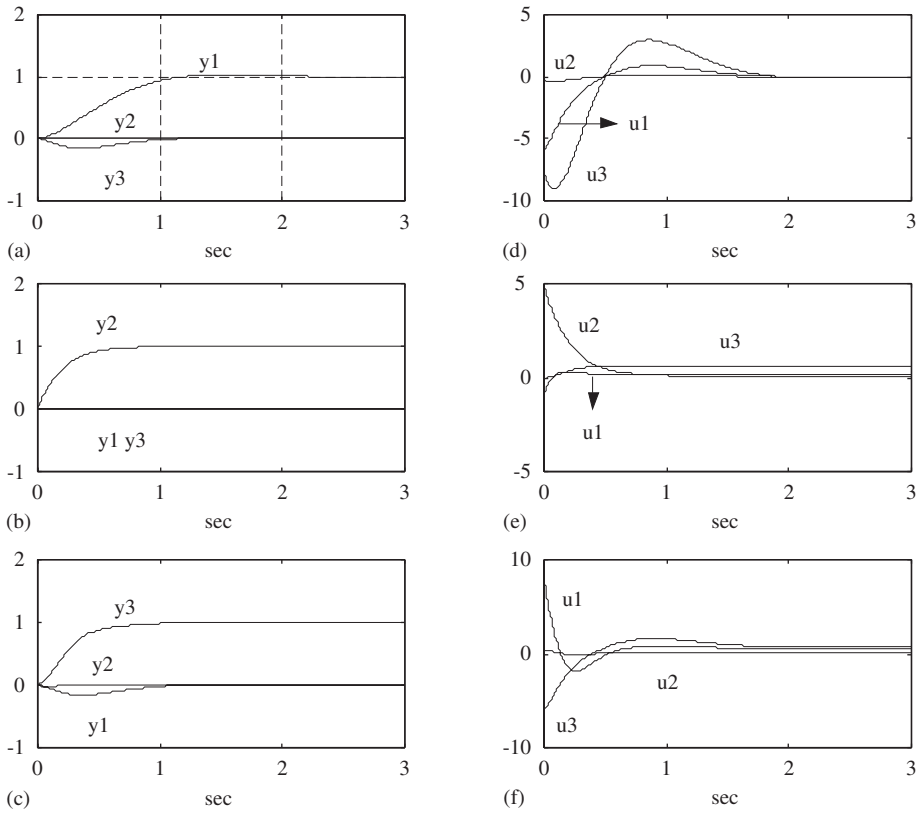

Figure 8. (a)–(c) Unit step responses for outputs and (d)–(f) control inputs.

The controller of the H_∞-LSDP is compared with the case of VS. Figure 9(a) and (b) show that the singular values of GK and KG for the H_∞-LSDP are almost the same as those for VS. Hence, the input and output sensitivity functions, which represent the ability to reject input and output disturbances, respectively, are almost the same for the two approaches. The largest peak values in Figure 10(a) and (b) are 1.59 and 1.57, respectively. These peak values also are almost the same as those of the second case.

Figure 12 shows the unit step responses for outputs and control inputs when the control scheme shown in Figure 11 is used for tracking. The overshoot of the outputs is less than 40%, the interaction between outputs is less than 30%, and the control inputs are limited as follows:

$$u_1 < 40^\circ, \quad u_2 < 10\,\mathrm{m/s}, \quad u_3 < 30^\circ$$

Hence, the VS case is the best for overshoots, interaction, and range of control input. Moreover, the VS case has a settling time about of 1 s, which is shorter than that of the H_∞-LSDP (≈ 2 s).

Because of the implementation difference with regard to the H_∞-LSDP and the VS, a pre-filter $F_p(s)$ is added for the H_∞-LSDP and the transfer function from r to y becomes

$$y = PK(I+PK)^{-1}F_p \cdot r = W_2^{-1}N_S Y_r W_2 F_p \cdot r \qquad (65)$$

The pre-filter is designed according to

$$F_p(s) = \mathrm{diag}\{pf, pf, pf\} \qquad (66)$$

where $pf = 8.454 \times 10^{-2} \cdot (s+59.142)/(s+5)$. The DC gain of pf is 1, and pf will cancel the farthest

DOI: 10.1002/rnc

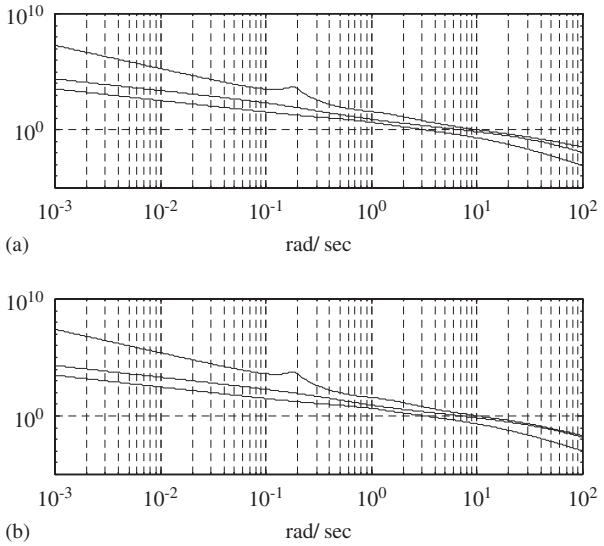

Figure 9. Singular values of (a) GK and (b) KG (LSDP).

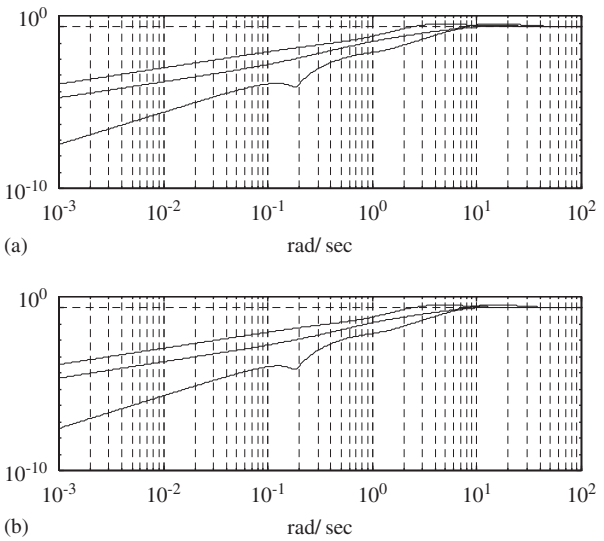

Figure 10. Singular values of (a) output sensitivity function and (b) input sensitivity function (LSDP).

pole of Y_r at -59.142 to improve the control effort. Hence, the function of $F_p(s)$ is similar to $H^{-1}(s)$ of

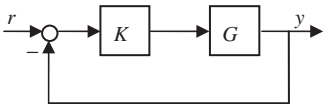

Figure 11. Control scheme for tracking.

Equation (62). Figure 13 shows the unit step responses for outputs and control inputs, and illustrates that the overshoot of the outputs is less than 30%, the interaction between outputs is less than 20%, and the control inputs are limited as follows:

$$u_1<3^\circ, \quad u_2<10\,\mathrm{m/s}, \quad u_3<20^\circ$$

$F_p(s)$ must be higher order to decrease the overshoot. Moreover, $F_p(s)$ is a phase-lag pre-filter. If Y_r (or N_S) has poles much farther than -59.142, the phase lag for the unit step response will be significant with respect to the pre-filter design of $F_p(s)$. However, the similar function with respect to $H(s)$ in VS does not have the phase-lag problem since $H(s)$ is in the feedback loop.

The stability margin of the H_∞-LSDP with or without a pre-filter is a little better than the VS case. Adding a pre-filter in the H_∞-LSDP can improve the control effort, interaction, and overshoot, but cannot improve the settling time due to the phase-lag pre-filter. The VS case seems the best design in many aspects, as summarized in Table I.

Example 2

This example presents the design of VS for a 2×2 nominal multiple-input multiple-output plant. W_2 is used to reject two channels of input and output unit step disturbances, and H is used to reject two channels of input and output sinusoidal disturbances at frequencies of 1 and 5 rad/s. In this case, the design can hardly be achieved using the H_∞-LSDP. The nominal plant is given by

$$G(s)=\frac{1}{s^2+9s+20}\begin{bmatrix}2 & -1\\ 0.5 & 3\end{bmatrix} \tag{67}$$

DOI: 10.1002/rnc

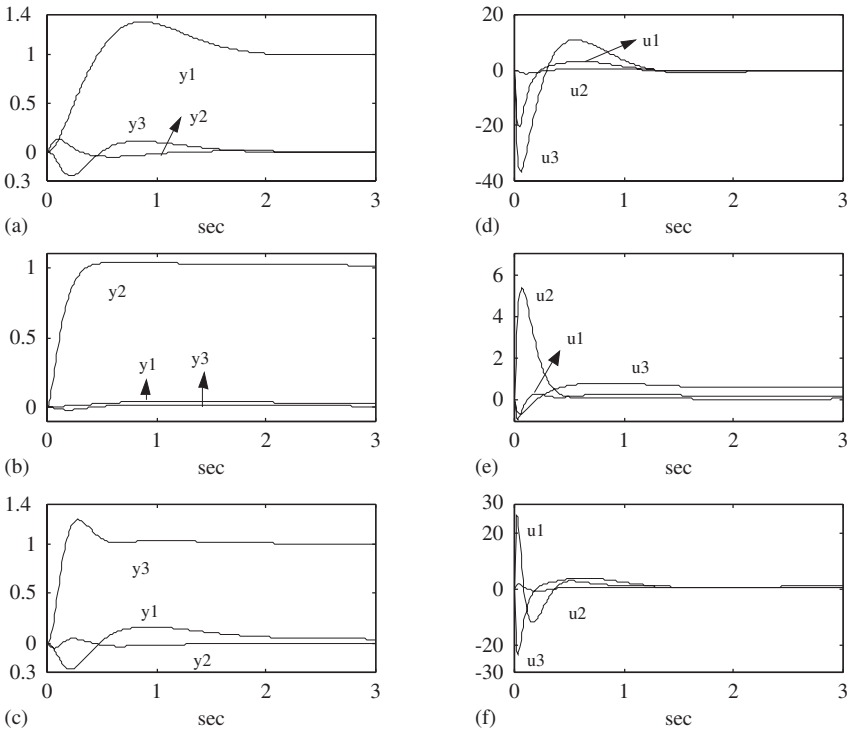

Figure 12. (a)–(c) Unit step responses for output responses and (d)–(f) control input responses (LSDP).

with the output vector (y_1, y_2). W_1 is an identity matrix and W_2 is given as

$$W_2 = \text{diag}\left\{\frac{45(s+0.1)}{s}, \frac{45(s+0.1)}{s}\right\} \tag{68}$$

Equation (68) yields two channels of input and output unit step disturbances with zero steady sate. Figure 14(a) and (b) show the singular values of G and the shaped plant W_2G, respectively.

The crossover frequency of W_2G in Figure 14(b) is about 10 rad/s. A controller K_∞ of Equation (18) satisfying Equation (13) ($\varepsilon = 0.549$) is obtained resulting in the observer composed of X_r and Y_r is obtained. When the input and output have multiple sinusoidal disturbances with frequencies at 1 and 5 rad/s, then according to Equations (48) and (53), the unimodular matrix H can be designed according to

$$\begin{aligned} H(s) = &\begin{bmatrix} -0.1894 & 0.0142 \\ 0.0142 & -0.3528 \end{bmatrix} \\ &+ \frac{1}{s+1}\begin{bmatrix} -1.6398 & -0.0319 \\ -0.0319 & -1.2732 \end{bmatrix} \\ &+ \frac{1}{(s+1)^2}\begin{bmatrix} 2.6995 & 0.0442 \\ 0.0442 & 2.1917 \end{bmatrix} \\ &+ \frac{1}{(s+1)^3}\begin{bmatrix} -2.4099 & -0.0323 \\ -0.0323 & -2.0381 \end{bmatrix} \end{aligned} \tag{69}$$

The output and input sensitivity functions are shown in Figure 15, where the peak value is 1.91. Moreover,

DOI: 10.1002/rnc

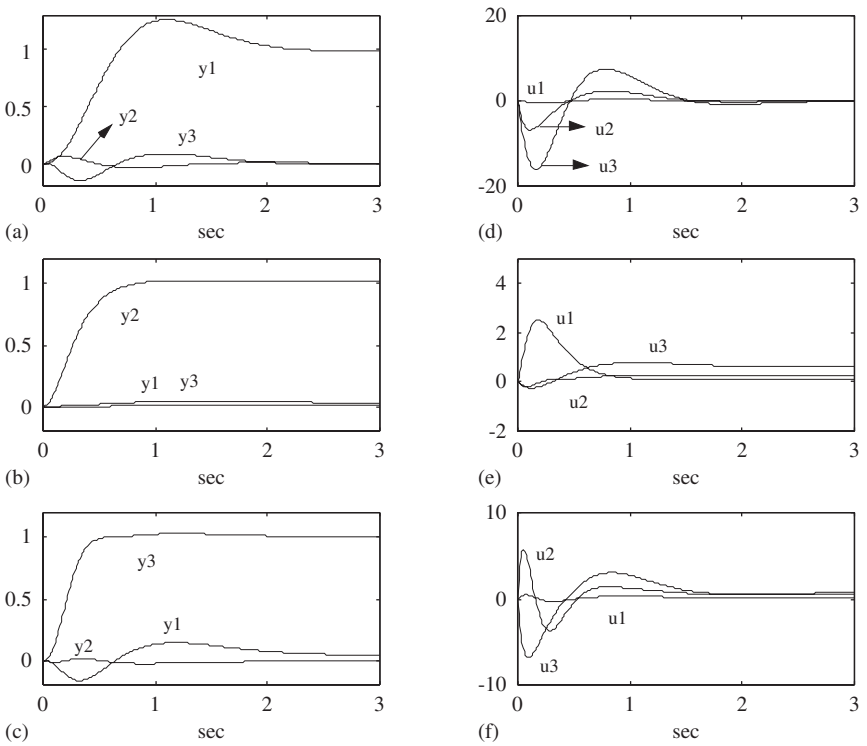

Figure 13. Unit step responses for output responses (a)–(c) and control input responses (d)–(f) (LSDP with pre-filter).

Table I. Comparison of VS and LSDP with/without pre-filter where $\bar{\varepsilon}$ is ε or ε_v, P_o and P_i are the peak values of the output and input sensitivity functions, respectively, and t_s is the settling time.

	$\bar{\varepsilon}$	P_o	P_i	u_1 (degree)	u_2 (m/s)	u_3 (degree)	Overshoot	Interaction	t_s (s)
VS	0.326	1.57	1.58	<8	<5	<10	No	<20%	1
LSDP	0.361	1.59	1.57	<40	<10	<30	<40%	<30%	2
LSDP with pre-filter	0.361	1.59	1.57	<3	<10	<20	<30%	<20%	2

the stability margin ε_v of the system is 0.190. Figure 16(a) shows the output responses for the disturbance vector $(1/s, 1/s)$ at the input and output of the plant. Figure 16(b) shows the output for the sinusoidal input disturbance vector $(\sin t + \sin 5t, \sin t + \sin 5t)$ at the input and output of the plant. Figure 16(c) shows the output responses for the total disturbances of Figure 16(a) and (b).

5. CONCLUSIONS

The YKP-like property of VS means that the VS design procedure can improve on the H_∞-LSDP while maintaining its inherent properties. Convenient numerical computation is not a feature of the VS design procedure because of the H parameter. However, H does give the VS design procedure flexibility in

DOI: 10.1002/rnc

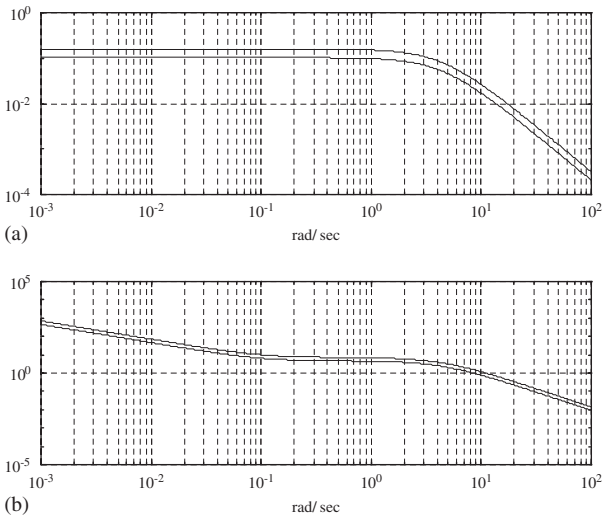

Figure 14. Singular values of (a) G and (b) W_2G.

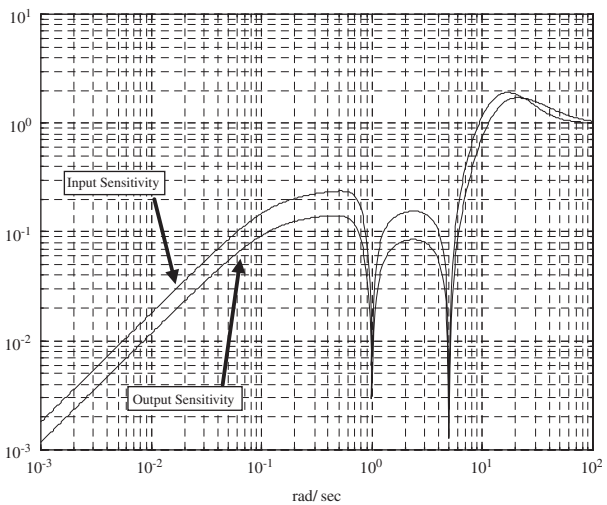

Figure 15. Output and input sensitivity functions of Example 2.

tracking control, or for the input-output step and known multiple sinusoidal disturbances. The tracking control in particular does not suffer from the phase-lag problem. The design of H requires more study to meet

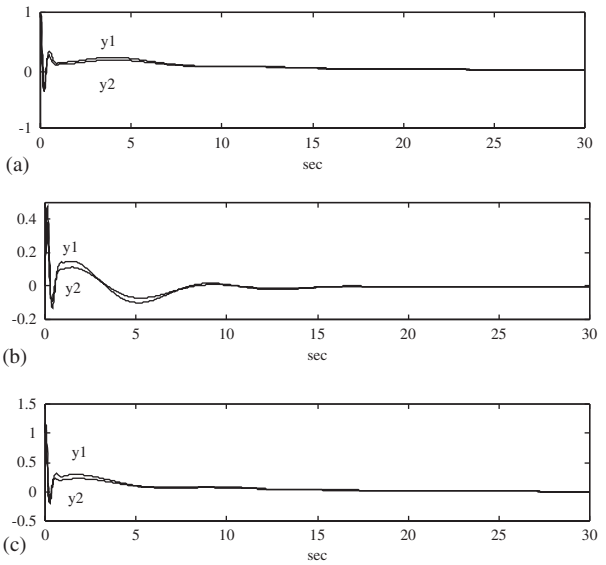

Figure 16. Output responses with respect to (a) the unit step disturbances $(1/s, 1/s)$ at the input and output and (b) the sinusoidal input disturbance $(\sin t+\sin 5t, \sin t+\sin 5t)$ at the input and output. (c) The total disturbances of (a) and (b).

the objectives of controlling disturbances and tracking simultaneously.

Demonstration files for Examples 1 and 2 are provided online at http://s-web.nctu.edu.tw/users/u9414829/WWW/.

APPENDIX A

A.1. Lower bound of the robust central controller

Theorem A.1 (*McFarlane and Glover* [*17*], *Theorem 3.1*).

A controller K_∞ satisfying Equation (13), where G_S is assumed to be square, also satisfies

$$\underline{\sigma}(K_\infty(\mathrm{j}\omega)) \geqslant \frac{\underline{\sigma}(G_S(\mathrm{j}\omega)) - (\gamma^2-1)^{1/2}}{\sqrt{\gamma^2-1}\,\underline{\sigma}(G_S(\mathrm{j}\omega)) + 1} \tag{A1}$$

for all ω such that

$$\underline{\sigma}(G_S(j\omega)) > \sqrt{\gamma^2-1}$$

where $\gamma = \varepsilon^{-1}$.

DOI: 10.1002/rnc

A.2. Upper bound of the robust central controller

Theorem A.2 (*McFarlane and Glover* [*17*], *Theorem 3.3*).
A controller K_∞ satisfying Equation (13), where G_S is assumed to be square, also satisfies

$$\bar{\sigma}(K_\infty(\mathrm{j}\omega)) \leqslant \frac{(\gamma^2-1)^{1/2}+\bar{\sigma}(G_S(\mathrm{j}\omega))}{1-\sqrt{\gamma^2-1}\bar{\sigma}(G_S(\mathrm{j}\omega))} \tag{A2}$$

for all ω such that

$$\bar{\sigma}(G_S(\mathrm{j}\omega)) < 1/\sqrt{\gamma^2-1}$$

where $\gamma=\varepsilon^{-1}$.

APPENDIX B

B.1. Bounds of standard closed-loop objectives

The following theorem is adapted from Theorem 4.2 in [17].

Theorem B.1
Suppose G is the nominal plant, and $K=W_1K_vW_2$ is the final (negative) output-feedback controller from the VS (see Figure 3). If

$$\|M_S^{-1}(I+K_vG_S)^{-1}[K_v \;\; I]\|_\infty \leqslant \gamma_v \tag{B1}$$

then

$$\bar{\sigma}(K(I+GK)^{-1}) \leqslant \gamma_v\bar{\sigma}(\tilde{M}_S)\bar{\sigma}(W_1)\bar{\sigma}(W_2) \tag{B2}$$

$$\bar{\sigma}((I+GK)^{-1}) \leqslant \min\{1+\gamma_v\bar{\sigma}(N_S)c(W_2), \gamma_v\bar{\sigma}(\tilde{M}_S)c(W_2)\} \tag{B3}$$

$$\bar{\sigma}(K(I+GK)^{-1}G) \leqslant \min\{1+\gamma_v\bar{\sigma}(M_S)c(W_1), \gamma_v\bar{\sigma}(\tilde{N}_S)c(W_1)\} \tag{B4}$$

$$\bar{\sigma}((I+GK)^{-1}G) \leqslant \frac{\gamma_v\bar{\sigma}(\tilde{N}_S)}{\sigma(W_1)\sigma(W_2)} \tag{B5}$$

$$\bar{\sigma}((I+KG)^{-1}) \leqslant \min\{\gamma_v\bar{\sigma}(M_S)c(W_1), 1+\gamma_v\bar{\sigma}(\tilde{N}_S)c(W_1)\} \tag{B6}$$

$$\bar{\sigma}(G(I+KG)^{-1}K) \leqslant \min\{\gamma_v\bar{\sigma}(N_S)c(W_2), 1+\gamma_v\bar{\sigma}(\tilde{M}_S)c(W_2)\} \tag{B7}$$

where $\gamma_v=\varepsilon_v^{-1}$; $(\tilde{N}_S, \tilde{M}_S)$ and (N_S, M_S) are a normalized LCF and RCF of $G_S(=W_2GW_1)$, respectively; $c(\bullet)$ denotes $\bar{\sigma}(\bullet)/\underline{\sigma}(\bullet)$, the condition number,

$$\bar{\sigma}(\tilde{N}_S)=\bar{\sigma}(N_S)=\left(\frac{\bar{\sigma}^2(W_2GW_1)}{1+\bar{\sigma}^2(W_2GW_1)}\right)^{1/2} \tag{B8}$$

and

$$\bar{\sigma}(\tilde{M}_S)=\bar{\sigma}(M_S)=\left(\frac{1}{1+\underline{\sigma}^2(W_2GW_1)}\right)^{1/2} \tag{B9}$$

Equations (B8) and (B9) are according to Lemma 4.1 in [18].

APPENDIX C

The state-space matrices of the aircraft model are

$$A=\begin{bmatrix} 0 & 0 & 1.1320 & 0 & -1.0000 \\ 0 & -0.0538 & -0.1712 & 0 & 0.0705 \\ 0 & 0 & 0 & 1.0000 & 0 \\ 0 & 0.0485 & 0 & -0.8556 & -1.0130 \\ 0 & -0.2909 & 0 & 1.0532 & -0.6859 \end{bmatrix}$$

$$B=\begin{bmatrix} 0 & 0 & 0 \\ -0.1200 & 1 & 0 \\ 0 & 0 & 0 \\ 4.4190 & 0 & -1.6650 \\ 1.5750 & 0 & -0.0732 \end{bmatrix}$$

$$C=\begin{bmatrix} 1 & 0 & 0 & 0 & 0 \\ 0 & 1 & 0 & 0 & 0 \\ 0 & 0 & 1 & 0 & 0 \end{bmatrix} \quad D=\begin{bmatrix} 0 & 0 & 0 \\ 0 & 0 & 0 \\ 0 & 0 & 0 \end{bmatrix}$$

DOI: 10.1002/rnc

APPENDIX D

1. Realization of X_r with $[A, B, C, D]$ for Example 1

$$A = \begin{bmatrix} -42.7680 & -1.4270 & 3.1844 & 0 & -1 & 0 & 0 & 0 \\ -1.4270 & -17.4481 & 3.1461 & 0 & 0.0705 & -0.3718 & 2.1909 & 0 \\ 2.0524 & 3.3173 & -69.2723 & 1 & 0 & 0 & 0 & 0 \\ 96.2007 & 49.0611 & -632.9635 & -.8556 & -1.0130 & 13.6918 & 0 & -5.1588 \\ 168.9301 & 21.6927 & -217.1787 & 1.0532 & -0.6859 & 4.8780 & 0 & -0.2268 \\ 16.0264 & 1.5231 & -11.0802 & 0 & 0 & 0 & 0 & 0 \\ 1.9211 & -2.8493 & -1.2976 & 0 & 0 & 0 & 0 & 0 \\ 31.9141 & .0024 & 22.6255 & 0 & 0 & 0 & 0 & 0 \end{bmatrix}$$

$$B = \begin{bmatrix} 0 & 0 & 0 \\ -2.8800 & 12.0000 & 0 \\ 0 & 0 & 0 \\ 106.0560 & 0 & -39.9600 \\ 37.8000 & 0 & -1.7568 \\ 3.0984 & 0 & 0 \\ 0 & 2.1909 & 0 \\ 0 & 0 & 3.0984 \end{bmatrix}$$

$$C = \begin{bmatrix} -0.6030 & -0.0916 & 0.6053 & 0.0708 & 0.1474 & 0.1276 & -0.0006 & -0.0015 \\ -0.0557 & 0.9904 & 0.0236 & 0.0082 & 0.0234 & -0.0007 & 0.1790 & -0.0017 \\ -0.7958 & -0.0313 & -1.0234 & -0.1524 & 0.3435 & 0.0002 & 0.0006 & 0.1287 \end{bmatrix}$$

$$D = \begin{bmatrix} 1 & 0 & 0 \\ 0 & 1 & 0 \\ 0 & 0 & 1 \end{bmatrix}$$

DOI: 10.1002/rnc

2. Realization of Y_r with $[A, B, C, D]$ for Example 1

A is the same as A of Appendix D.1.

$$B = \begin{bmatrix} 42.7680 & 1.4270 & -2.0524 \\ 1.4270 & 17.3943 & -3.3173 \\ -2.0524 & -3.3173 & 69.27230 \\ -96.2007 & -49.0126 & 632.9635 \\ -168.9301 & -21.9836 & 217.1787 \\ -16.0264 & -1.5231 & 11.0802 \\ -1.9211 & 2.8493 & 1.2976 \\ -31.9141 & -0.0024 & -22.6255 \end{bmatrix}$$

C is the same as C of Appendix D.1.

$$D = \begin{bmatrix} 0 & 0 & 0 \\ 0 & 0 & 0 \\ 0 & 0 & 0 \end{bmatrix}$$

3. Realization of M_S with $[A, B, C, D]$ for Example 1

$$A = \left[\begin{array}{cccccccc} 0 & 0 & 1.1320 & 0 & -1 & 0 & 0 & 0 \\ -1.0689 & -12.2025 & 1.2885 & 0.1056 & 0.2145 & 0.0038 & 0.0412 & 0.1498 \\ 0 & 0 & 0 & 1 & 0 & 0 & 0 & 0 \\ 32.1579 & 8.5154 & -105.1063 & -14.4611 & -2.9165 & 0.1674 & 0.0920 & 0.1498 \\ 21.3971 & 3.1176 & -24.6786 & -1.9826 & -5.6525 & 0.05659 & 0.02497 & 0.0579 \\ 1.8685 & 0.2839 & -1.8754 & -0.2195 & -0.4566 & -0.3954 & 0.0020 & 0.0048 \\ 0.1219 & -2.1699 & -0.0518 & -0.0180 & -0.0512 & 0.0015 & -0.3921 & 0.0037 \\ 2.4656 & 0.09697 & 3.1722 & 0.4723 & -1.0641 & -0.0008 & -0.0019 & -0.3989 \end{array}\right]$$

$$B = \begin{bmatrix} 0 & 0 & 0 \\ -2.8800 & 12 & 0 \\ 0 & 0 & 0 \\ 106.0560 & 0 & -39.9600 \\ 37.8000 & 0 & -1.7568 \\ 3.0984 & 0 & 0 \\ 0 & 2.1909 & 0 \\ 0 & 0 & 3.0984 \end{bmatrix}$$

C is the negative C of Appendix D.1

$$D = \begin{bmatrix} 1 & 0 & 0 \\ 0 & 1 & 0 \\ 0 & 0 & 1 \end{bmatrix}$$

ACKNOWLEDGEMENTS

This study was supported by the Republic of China National Science Council under contract number NSC 95-2221-E-009-181.

DOI: 10.1002/rnc

REFERENCES

1. Wolovich WA. *Linear Multivariable Systems*. Springer: New York, 1974.
2. Chen CT. *Linear System Theory and Design*. Oxford University Press: New York, 1984.
3. Giua A, Sanna M, Seatzu C. Observer–controller design for three dimensional overhead cranes using time-scaling. *Mathematical and Computer Modeling of Dynamical Systems* 2001; **7**(1):77–107.
4. Pandian SR, Takemura F, Hayakawa Y, Kawamura S. Pressure observer–controller design for pneumatic cylinder actuators. *IEEE-ASME Transactions on Mechatronics* 2002; **7**(4): 490–499.
5. Noijen SPM, Lambrechts PF, Nijmeijer H. An observer–controller combination for a unicycle mobile robot. *International Journal of Control* 2005; **78**(2):81–87.
6. Driessen BJ, Duggirala VM. Globally asymptotic and locally exponential tracking observer/controller for a relatively large class of systems with hysteresis. *Journal of Intelligent and Robotic Systems* 2007; **50**:207–215.
7. Alazard D, Apkarian P. Exact observer-based structures for arbitrary compensators. *International Journal of Robust and Nonlinear Control* 1999; **9**(2):101–118.
8. Gao ZW, Ho DWC. Comments on parameterization of stabilization compensators by using reduced-order observers. *IEEE Transactions on Automatic Control* 2001; **46**(11): 1840–1842.
9. Gao ZW, So ATP. A general doubly coprime factorization for descriptor systems. *Systems and Control Letters* 2003; **49**(3):213–224.
10. Gao ZW. PD observer parameterization design for descriptor systems. *Journal of the Franklin Institute-Engineering and Applied Mathematics* 2005; **342**(5):551–564.
11. Viswanadham N, Vidyasagar M. Stabilization of linear and nonlinear dynamical systems using an observer–controller configuration. *Systems and Control Letters* 1981; **8**(2):87–91.
12. Vidyasagar M. *Control System Synthesis*: *A Coprime Factorization Approach*. MIT Press: Cambridge, MA, 1985.
13. Kucera V. *Discrete Linear Control*: *The Polynomial Equation Approach*. Wiley: New York, 1979.
14. Youla DC, Jabr HA, Bongiorno JJ. Modern Wiener–Hopf design of optimal controllers—Part II: the multivariable case. *IEEE Transactions on Automatic Control* 1976; **21**(3): 319–338.
15. Kucera V. Stability of discrete linear feedback systems. *Proceedings of the IFAC World Congress*, Boston, MA, 1975; **44**(1).
16. Glover K, McFarlane D. Robust stabilization of normalized coprime factor plant descriptions with H_∞-bounded uncertainty. *IEEE Transactions on Automatic Control* 1989; **34**(8):821–830.
17. McFarlane D, Glover K. *Robust Controller Design Using Normalized Coprime Factor Plant Descriptions*. Lecture Notes in Control and Information Sciences, vol. 138. Springer: New York, 1990.
18. McFarlane D, Glover K. A loop shaping design procedure using H_∞ synthesis. *IEEE Transactions on Automatic Control* 1992; **37**(6):759–769.
19. Panagopoulos H, Astrom KJ. PID control design and H_∞ loop shaping. *Proceedings of the 1999 IEEE International Conference on Control Applications*, vol. 1(1), 1999; 103–108.
20. Reinelt W. Loop shaping of multivariable systems with hard constraints on the control signal. *Electrical Engineering* 2001; **83**(4):169–177.
21. Zhu CJ, Khammash M, Vittal V, Qiu WZ. Robust power system stabilizer design using H_∞ loop shaping approach. *IEEE Transactions on Power Systems* 2003; **18**(2): 810–818.
22. Schinstock DE, Wei ZH, Yang T. Loop shaping design for tracking performance in machine axes. *ISA Transactions* 2006; **45**(1):55–66.
23. Patra S, Sen S, Ray G. Design of robust load frequency controller: H_∞ loop shaping approach. *Electric Power Components and Systems* 2007; **35**(7):769–783.
24. Huang YY, Lee AC. Generalized of all stabilizing compensators for finite-dimensional linear systems. *Journal of the Franklin Institute* 2007; **344**(8):1075–1090.
25. Vidyasagar M. The graph metric for unstable plants and robustness estimates for feedback stability. *IEEE Transactions on Automatic Control* 1984; **29**(5):403–418.
26. Vidyasagar M, Kumira H. Robust controllers for uncertain linear multivariable systems. *Automatica* 1986; **22**(1): 85–94.
27. Georgiou TT, Smith MC. Optimal robustness in the gap metric. *IEEE Transactions on Automatic Control* 1990; **35**(6): 673–686.

DOI: 10.1002/rnc